Modeling banded vegetation patterns in semiarid regions: Interdependence between biomass growth rate and relevant hydrological processes

N. Ursino[1]

Received 28 June 2006; revised 24 October 2006; accepted 6 November 2006; published 10 April 2007.

[1] Vegetation patterns, such as regular spots and bands, have been observed in arid and semiarid lands. One of the most common explanations for vegetation banding is that the homogeneous steady state solution of soil moisture and vegetation biomass density balance, expressed in the form of a bucket model, may be unstable under conditions of scarce mean annual rainfall. Even though the theory seems to support our intuitive explanation of the phenomenon, there are still unresolved questions concerning soil parameterization, relevant hydrological processes, and the way plant physiology should be modeled in arid and semiarid environments where vegetation patterns have been observed. This paper examines the interrelation between hydrological processes and plant physiology. The biomass growth rate resembles plant physiology within the bucket model and determines the survival plant strategy given a limited soil moisture availability. The fact that very different hypotheses concerning the biomass growth rate have been formulated has not yet been given the important consideration it deserves. Different models for vegetation banding will be considered here. They are formulated by introducing different growth rates within the same soil moisture and vegetation balance equations. Linear stability analysis and numerical integration of the different models showed some relevant interrelation between hydrological and physiological features. It was demonstrated that the relation between biomass growth rate and biomass density determines which hydrological process enables vegetation pattern initiation. The discussion of this result leads to a critical review of previously published hypotheses on plant physiology and hydrological processes inducing vegetation organization.

Citation: Ursino, N. (2007), Modeling banded vegetation patterns in semiarid regions: Interdependence between biomass growth rate and relevant hydrological processes, *Water Resour. Res.*, *43*, W04412, doi:10.1029/2006WR005292.

1. Introduction

[2] Densely vegetated stripes alternating with bare soil (banded vegetation patterns) occur in arid and semiarid lands, mainly on gentle slopes, apparently regardless of soil heterogeneity [*Worral*, 1959, 1960; *Boaler and Hodge*, 1964, *White*, 1970, 1971; *Tongway and Ludwig*, 1990]. Indeed, their establishment seems to be due to a small-scale process of water redistribution by runoff [*Boaler and Hodge*, 1962; *Valentin et al.*, 1999; *Fernando and Cortina*, 2002].

[3] One of the most commonly accepted explanations for vegetation banding is that the homogeneous steady state solution of the soil moisture and vegetation biomass density balance, expressed in the form of a bucket model, may be unstable under conditions of scarce mean annual rainfall (below 750 mm yr^{-1}). Similar results have been found by coupling the soil moisture and biomass balance to a third equation to describe surface water or nutrient dynamics [*Rietkerk et al.*, 2004]. Many environmental scientists have investigated the processes of banded vegetation pattern formation due to diffusion-driven instability. *Lefever and Lejeune* [1997] model short-range competitive interactions controlling plant reproduction and long-range competition for environmental resources, demonstrating the instability of the biomass balance equation. *Klausmeier* [1999] and *Von Hardenberg et al.* [2001] propose models for biomass and soil moisture balance leading to reaction-diffusion-type instability [*Turing*, 1952; *Murray*, 1989]. *HilleRisLambers et al.* [2001] and *Gilad et al.* [2004] analyze the stability of a model for soil moisture, biomass and surface water, considering the feedback between surface water infiltration and biomass density. Few studies focus on how soil characteristics, geomorphology, and time variability of hydrological forcing affect the organization of the vegetation in patterns, notwithstanding these are key elements of the ecohydrology balances. *Ursino* [2005] extends the model of *Klausmeier* [1999] in order to account for soil properties, and *Ursino and Contarini* [2006] evaluate the effect of rainfall seasonality and daily variability on the stability of the same model.

[4] *Rietkerk et al.* [2004] present a comprehensive review on models for self-organized patchiness in different ecosys-

[1]Dipartimento di Ingegneria Idraulica, Marittima, Ambientale e Geotecnica, University of Padova, Padua, Italy.

0043-1397/07/2006WR005292$09.00

tems (namely, arid land, savannas, and peatland). In their review paper, the authors point at the relevance of the phenomenon of "*bistability*", resulting in observable vegetation patchiness. Since vegetation patterns are envisioned as indicators that the ecosystem is evolving toward non reversible, sudden shifts, the authors foresee the possibility that further research could bridge the gap between theory, observation and management, creating models for early warning and restoration.

[5] An additional strong motivation for studying how vegetation bands develop and persist, is provided by *Valentin et al.* [1999]. They remark that banded vegetation patterns optimize biomass production, limit land degradation and are highly self sustainable. Thus "profound lessons can be learnt from the study of banded landscapes in terms of ecosystem functions. When designing water-harvesting systems or restoring degraded arid land, banded vegetation patterns should be imitated to optimize biomass production and limit land degradation" [*Valentin et al.*, 1999, p. 2].

[6] Beyond the fascinating explanation provided by stability analysis, it is evident that there is more than one reason to attempt the development of realistic models that could further the understanding and prediction of relevant ecological and hydrological processes for vegetation patterns. One way to enhance the predictive capability of models for vegetation patterning and to extend their applicability to restoration projects or agriculture management is to undertake the critical revision of the biological and hydrological processes that are mimicked by different models. The effective parameters that appear within the models must be supported by a coherent physically based explanation, since they often account for lower-scale processes that are not explicitly resolved but could be measured or predicted independently.

[7] There are still unresolved questions concerning soil parameterization, relevant hydrological processes and the way plant physiology should be modeled in arid and semiarid environments where vegetation patterns have been observed. *Ursino* [2005] on the basis of the stability analysis of her extended version of the Klausmeier's model [*Klausmeier*, 1999], demonstrates that effective soil parameters might indeed lead to numerical results that fit well with the experimental data on the threshold gradient slope below which vegetation bands are not observed. Nevertheless, whether these effective parameters could be physically supported is unclear. Indeed, the parameters used by *Ursino* [2005] to fit the experimental data seem to be beyond their usual range of variability as the author indicates. The extended model did not account for the feedback between soil moisture and vegetation density that *HilleRisLambers et al.* [2001] and *Gilad et al.* [2004] indicate as a process of utmost importance for vegetation patterning. Whether including the feedback within the extended model may eliminate the need for unrealistic soil parameterization certainly deserves careful investigation. An even more important fact emerging as a result of a careful literature review is the following: the original model of *Klausmeier* [1999] as well as its extended version [*Ursino*, 2005], the model of *HilleRisLambers et al.* [2001] and the one of *Gilad et al.* [2004] are based on three different assumptions concerning the biomass growth rate. The fact that very different hypotheses concerning the biomass growth rate have been formulated, has not yet been given the consideration it deserves. The biomass growth rate resembles plant physiology within the model and determines the survival plant strategy under water scarcity conditions. This paper focuses on the interrelation between hydrological processes and plant physiology, testing different definitions of the biomass growth rate within the same model for vegetation banding. As a consequence, this model shares features with the different models that have been referred to above, depending on the specification of the growth rate. This modeling exercise results first of all in a critical review of previous published hypotheses on hydrological processes inducing vegetation organization and plant physiology. Secondly, it illustrates how hydrological and physiological features are strongly interrelated. More specifically, it attempts to provide an answer to the question: depending on plant physiology, which hydrological process achieves more relevance, and why?

[8] The model for soil moisture, biomass and surface water accounting explicitly for soil processes (with consideration given for feedback between surface water infiltration and biomass density), is presented and discussed in section 2.1. Different biomass growth rates are hypothesized (section 2.2) and the problem of linear stability analysis is solved analytically and repeatedly for any growth rate model. The three independent variables of the problem (soil moisture, biomass and surface water) are supposed to have a diffusive behavior and thus the problem will typically exhibit Turing like instability, predicting vegetation pattern initiation (a summary on linear stability analysis was presented in section 2.3). In section 3.1 it is demonstrated that between soil moisture diffusion and surface water redistribution only one or both processes have a major impact on the stability field of the model's steady state solution, depending on the functionality of the biomass growth, and thus ultimately, depending on plant physiology. The long-term solution of the problem is explored by numerical integration, discovering some questionable results (section 3.2) beyond the successful outcome of the stability analysis. In section 4 the results are discussed.

2. Theory

2.1. Model

[9] The model for soil moisture (W) plant biomass (N) and surface water (O) balance is defined on an infinite one dimensional domain indexed by X as a function of time T, as follows:

$$\begin{aligned}
\frac{\partial W}{\partial T} &= \alpha O \frac{N + K_2 k_3}{N + K_2} - LW - F(W,N) + V_W \frac{\partial W}{\partial X} + D_W \frac{\partial^2 W}{\partial X^2} \\
\frac{\partial N}{\partial T} &= JF(W,N) - MN + D_N \frac{\partial^2 N}{\partial X^2} \\
\frac{\partial O}{\partial T} &= A - \alpha O \frac{N + K_2 k_3}{N + K_2} + V_O \frac{\partial O}{\partial X} + D_O \frac{\partial^2 O}{\partial X^2}
\end{aligned} \tag{1}$$

Model (1) does not take explicitly into account the transport of nutrients even if it may have an influence on stability [*Rietkerk et al.*, 1997]. Furthermore, model (1) is based on the simplistic hypothesis of uniform net rainfall A, in order to obtain more easily an analytical solution of the linear

Table 1. Relative Growth Rates and Parameter Values

		Parameters	
	Growth Rate $\frac{1}{n}\frac{dn}{dt}$	Growth Rate Function	Model
Case 1	$-m\left(1-\frac{rw}{m}n\right)$	$m = 0.45$ $r = 0.36$ $k_2 = 10$	$L = 4\ \mathrm{yr}^{-1}$, $J = 0.003\ \mathrm{kg\ m^{-2}\ mm^{-1}}$ $M = 1.8\ \mathrm{yr}^{-1}$, $K_2 = 0.005\ \mathrm{kg\ m^{-2}}$ $\theta_s = 0.4$, $W_s = 40$ mm, $\alpha = 10\ \mathrm{m}^{-1}$ $\ell = 1$, $D_N = 4\ \mathrm{m^2\ yr^{-1}}$
Case 2	$g\frac{w}{k_1+w} - \mathrm{m}$	$g = 5$ $k_1 = 0.075$ $m = 2.74$ $k_2 = 0.0125$	$L = 36\ \mathrm{yr}^{-1}$, $J = 0.01\ \mathrm{kg\ m^{-2}\ mm^{-1}}$ $M = 100\ \mathrm{yr}^{-1}$, $K_2 = 0.005\ \mathrm{kg\ m^{-2}}$ $\theta_s = 0.4$, $W_s = 40$ mm, $\alpha = 10\ \mathrm{m}^{-1}$ $\ell = 1$, $D_N = 4\ \mathrm{m^2\ yr^{-1}}$
Case 3			$L = 4\ \mathrm{yr}^{-1}$, $J = 0.003\ \mathrm{kg\ m^{-2}\ mm^{-1}}$
Case 3.1	$b\left(1-\frac{n}{k'_n w}\right)$	$b = 2$ $k'_n = 10$	$K_2 = 0.005\ \mathrm{kg\ m^{-2}}$ $\theta_s = 0.4$, $W_s = 40$ mm, $\alpha = 10\ \mathrm{m}^{-1}$
Case 3.2	$b'w\left(1-\frac{n}{k_n}\right)$	$b' = 2$ $k_n = 10$ $k_2 = 10$	$\ell = 1$, $D_N = 4\ \mathrm{m^2\ yr^{-1}}$

stability problem. The impact of seasonality and rainfall shower frequency have been discussed by *Ursino and Contarini* [2006], and (also) on the basis of their results, it may be stated here that a more realistic hypothesis on net rainfall would not change the main conclusions reported in this paper, even though it clearly has an impact on the results.

[10] The net rainfall A infiltrates preferentially where plants grow, inducing a feedback mechanism that is accounted for by the term $\alpha O \frac{n+k_2k_3}{n+k_2}$, where K_2 depends on the rate at which surface water infiltration increases with biomass density, $\alpha\ O\ k_3$ is the minimum infiltration rate of surface water in the absence of plants and $\alpha\ O$ is the maximum infiltration rate [*Rietkerk et al.*, 1997; *HilleRisLambers et al.*, 2001]. LW is the water loss due to evaporation and leakage, that may be approximated with a linear function of the soil moisture under stress conditions [*Rodriguez-Iturbe et al.*, 1999; *Salvucci*, 2001]. Close to saturation, it reaches an upper limit that is ignored here to allow the analytical solution of the problem. This hypothesis has a minor impact on the results (see, e.g., the sensitivity analysis reported by *Ursino and Contarini* [2006]) in the cases examined here. MN is the plant biomass loss due to mortality; D_W and V_W represent the soil moisture diffusion coefficient and transverse velocity; J is the yield of plant biomass per unit water consumed; D_N is the diffusion coefficient of plant dispersal, and $F(W, N)$ is the plants water uptake. $JF(W, N) - MN$ represents the growth rate of homogeneous vegetation. Different growth rate functions will be considered and discussed in the following Subsection. The following expression for the net variation of soil moisture due to horizontal flux q: $-\frac{dq}{dX} = D_W \frac{d^2\theta}{dX^2} + V_W \frac{d\theta}{dX}$, may be obtained by combining Richards equation [*Richards*, 1931] that governs the vadose zone water flow and Gardner's exponential relations for unsaturated conductivity $K(\theta)$ and soil moisture content θ [*Gardner*, 1958]: $K(\theta) = K_s e^{(\alpha\Psi)}$ and $\theta = \theta_s\ e^{(\alpha\Psi)}$, where Ψ is the negative pressure head and θ_s is the saturated soil moisture content. W and Q are defined here as the averaged q and θ over the root zone depth H. Assuming that the net horizontal variation of Q equals the time variation of W minus the net vertical soil moisture flux (the letter is due to rainfall infiltration, plant uptake, evapotranspiration and leakage) the first of (1) is demonstrated. Then, V_W and D_W might be expressed as functions of the saturated conductivity K_s and the inverse of the capillary rise α only: $V_W = i \cdot K_s\theta_s^{-1}$ and $D_W = K_s(\theta_s \cdot \alpha)^{-1}$, where $i = dZ/dX$ is the soil gradient slope [see also *Ursino*, 2005]. Viscous flow equation of a shallow surface water layer with uniform vertical distribution of velocity U is $U \propto -\frac{d(O+Z)}{dX}$. By substituting this expression within the surface water balance equation $\frac{\partial O}{\partial t} + \frac{\partial OU}{\partial X}$ = precipitation - infiltration and neglecting $\left(\frac{\partial O}{\partial X}\right)^2$, leads to the third equation in model (2) that is a linearized version of the surface water balance equation proposed by *Gilad et al.* [2004]. Neglecting $\left(\frac{\partial O}{\partial X}\right)^2$ has negligible influence on the final results presented here, as it was verified by solving numerically (2) (not shown here). D_O and V_O are the surface water diffusion coefficient and transverse velocity, and are linked by the following equation: $V_O = \frac{iDO}{O}$. V_W and V_O, of course, vanish on flat ground where the vegetation patterns do not develop in any preferential direction and thus they are expected to be spots rather than bands. Nevertheless, the results of the stability analysis hold true on flat ground as well.

[11] Model (1), may be conveniently expressed in dimensionless form:

$$\begin{aligned}
\frac{\partial w}{\partial t} &= \ell o \frac{n+k_2k_3}{n+k_2} - w - f(w,n) + v_w\frac{\partial w}{\partial x} + d_w\frac{\partial^2 w}{\partial x^2}\\
\frac{\partial n}{\partial t} &= f(w,n) - mn + d_n\frac{\partial^2 n}{\partial^2 x}\\
\frac{\partial o}{\partial t} &= a - \ell o\frac{n+k_2k_3}{n+k_2} + v_o\frac{\partial o}{\partial x} + d_o\frac{\partial^2 o}{\partial x^2}
\end{aligned} \tag{2}$$

where $t = LT$, $x = D_W^{-1/2}L^{1/2}X$, $w = W_s^{-1}W$ $n = (W_sJ)^{-1}N$, $o = W_s^{-1}O$, $\ell = \alpha\ L^{-1}$, $k_2 = (W_sJ)^{-1}K_2$, $m = L^{-1}M$, and $a = (LW_s)^{-1}A$. W_s represents the soil moisture storage capacity that is approximately $W_s = \theta_s\ H$. H is the soil depth where the root uptake occurs and θ_s is the saturated soil moisture content. Furthermore, $f(w, n) = W_s^{-1}\ LF(W_s \cdot w, W_sJ \cdot n)$, $v_w = V_W(LD_W)^{-1/2}$, $v_o = V_O\,(LD_W)^{-1/2}$ $d_w = 1$, $d_n = D_ND^{-1/2}{}_W$, and $d_o = D_OD_W^{-1/2}$.

2.2. Biomass Growth Rates

[12] Three different hypotheses on $f(w, n)$ have been formulated. Mathematical formulations and parameters are taken from literature and summarized in Table 1. In case study 1, model (2) may be interpreted as an extended

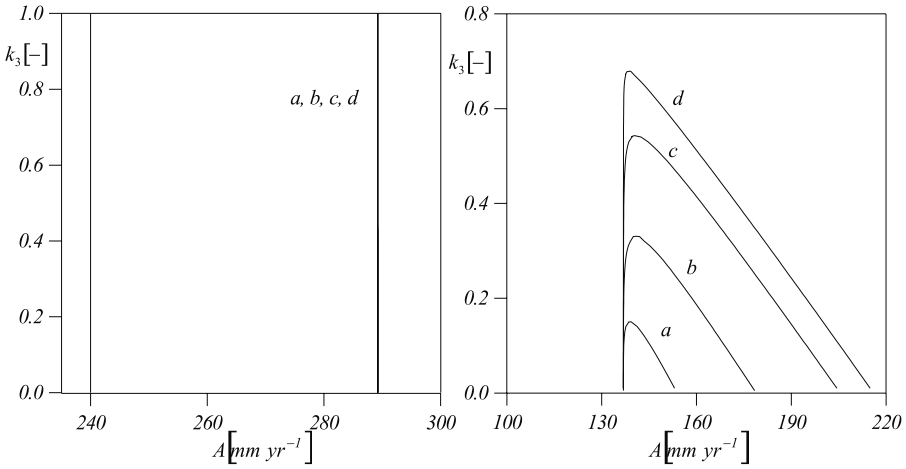

Figure 1. Critical stability condition (7) plotted on the $k_3 - A$ plane for different values of D_O. (left) Case study 1. (right) Case study 2. Here: a, $D_0 = 4 \times 10^1$ m^2 yr^{-1}; b, $D_0 = 4 \times 10^2$ m^2 yr^{-1}; c, $D_0 = 4 \times 10^3$ m^2 yr^{-1}; d, $D_0 = 4 \times 10^4$ m^2 yr^{-1}.

version of the model of *Klausmeier* [1999] where the surface water balance is added and the positive feedback between vegetation density and water infiltration is taken into account. In case study 2, model (2) resembles the model of *HilleRisLambes et al.* [2001], where the lateral surface water flow is modeled according to *Gilad et al* [2004]. *Klausmeier* [1999] and *HilleRisLambes et al.* [2001] proposed different parameters' values for problem (1) (see Table 1). It was necessary to set m, r, g k_1 and k_2 accordingly in order to find physically meaningful steady state solutions. In case study 3.1 and 3.2, $f(w, n)$ was expressed as a self limiting process assuming the form of the logistic growth rate introduced by *Verhulst* [1838] that has been an object of recent discussion [*Olson*, 1992; *Berryman*, 1992; *Young*, 1992; *Tsoularis and Wallace*, 2002; *Gabriel et al.*, 2005]. In case studies 3.1 and 3.2, a soil-moisture-dependent growth rate was obtained by expressing the carrying capacity of the population as $k'_n w$ (case 3.1) and by determining that the temporal response of the system was $b'w$ (case 3.2).

[13] At a first glance, the expression for $f(w, n)$ in case study 1, may seem to resemble some of the features of the logistic model: there are two homogeneous equilibrium states, one of them is the bare soil, while the growth rate is a linear function of n. Nevertheless, in case 1, $f(w, n)$ differs substantially from the logistic growth model because the parameters b and $b'w$ that regulate the temporal response of the system, are always positive, whereas the corresponding $-m$ that regulates the temporal response of the system in case study 1 is always negative. In case 1, the relative growth rate of uniform vegetation $\frac{dn}{dt}\frac{1}{n}$, always increases with n, attaining a minimum at $n = 0$. Opposite, in cases study 3.1 and 3.2 it attains a maximum at $n = 0$ and decreases for increasing n. *Gilad et al.* [2004] used the logistic equation within a differential problem similar to (2) with additional mortality and saturation-dependent b as in case 3.2, whereas, for the soil moisture consumed by plants ($f(w, n)$ in the first of (2)) the authors adopt a different simplified expression. These discrepancies make the com-

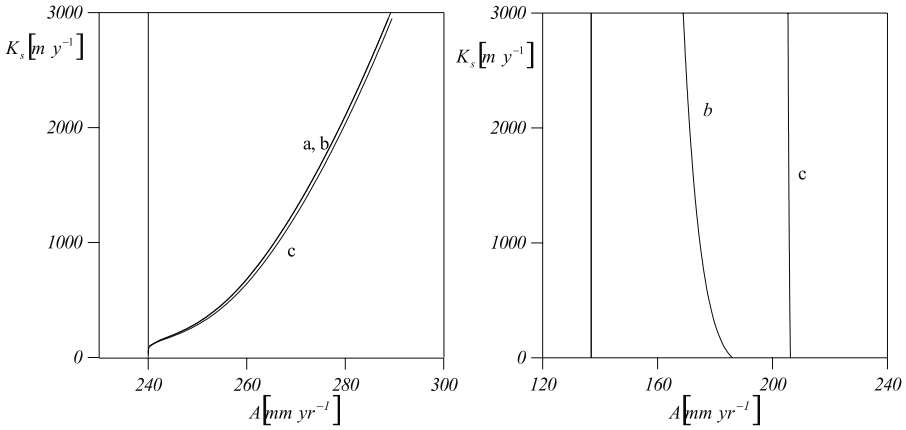

Figure 2. Critical stability condition (7) plotted on the $K_s - A$ plane for different values of D_O. (left) Case study 1. (right) Case study 2. Here: a, $D_0 = 4 \times 10^0$ m^2 yr^{-1}; b, $D_0 = 4 \times 10^2$ m^2 yr^{-1}; c, $D_0 = 4 \times 10^4$ m^2 yr^{-1}.

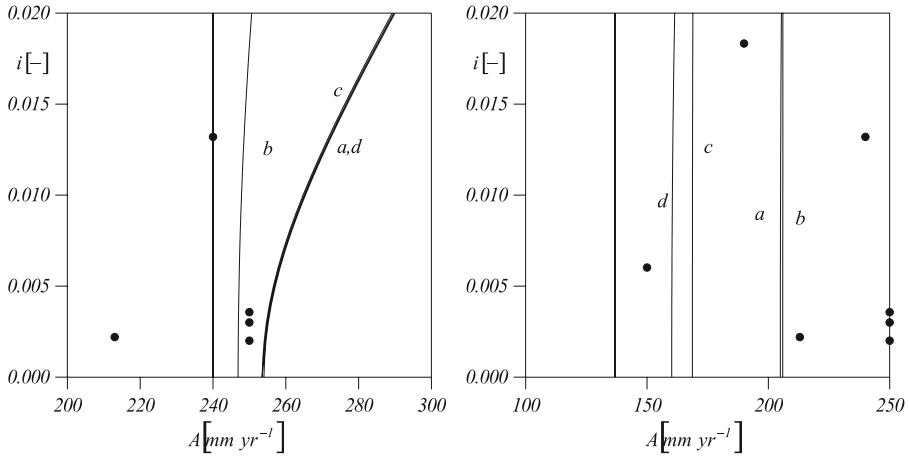

Figure 3. Critical stability condition (7) plotted on the $i - A$ plane for different values of D_O. (left) Case study 1. (right) Case study 2. Here: a, base; b, reduced soil moisture diffusion; c, reduced surface layer diffusion; d, reduced feedback. Parameter values are reported in Table 2.

parison between (2) and their model not very straight forward.

[14] Models such as exponential growth, characterized by a constant relative growth rate (case study 2) imply that the population may grow exponentially with no limitation, and this hypothesis may not be acceptable when competition for limited resources comes into play. Similar consideration may be reserved for case study 1. Case study 1 and 2 mimic local cooperative interaction among plants, whereas in case 3, local competition for environmental resources is modeled. Plant cooperation may be expected to take place in semiarid environments when vegetation patterning initiates. Nevertheless, in the long term, resource scarcity is expected to limit the vegetation density directly through the growth rate. By approaching the problem of vegetation patterning by linear stability analysis, just the short-term response of the ecosystem to a small heterogeneous perturbation is investigated. In other words, we are studying the band initiation rather than the band evolution. As a consequence, in this framework, the expressions for $f(w, n)$ chosen in cases 1 and 2 may lead to acceptable results.

2.3. Linear Stability Analysis

[15] The stability of the steady state solution (w_0, n_0, o_0) of (2) was tested by linearizing the problem about (w_0, n_0, o_0). For a small perturbation

$$u = \begin{pmatrix} w - w_0 \\ n - n_o \\ o - o_o \end{pmatrix} \tag{3}$$

in the form

$$u = \sum_k c_k e^{\lambda t} U_k(x). \tag{4}$$

[16] The eigenvalue λ represents the growth rate of the disturbance and the constants c_k are determined by a Fourier expansion of the perturbation in terms of $U_k(x)$. Substituting (4) into (2) leads to the following relation

$$u_t = Au + V\nabla u - D\nabla^2 u, \tag{5}$$

where

$$A = \begin{pmatrix} l_w & l_n & l_o \\ h_w & h_n & h_o \\ t_w & t_n & t_o \end{pmatrix}, \; V = \begin{pmatrix} v_w & 0 & 0 \\ 0 & 0 & 0 \\ 0 & 0 & v_o \end{pmatrix},$$
$$D = \begin{pmatrix} d_w & 0 & 0 \\ 0 & d_n & 0 \\ 0 & 0 & d_o \end{pmatrix}; \tag{6}$$

with $\ell = \ell o \frac{n + k_2 k_3}{n + k_2} - w - f(w, n)$, $h = f(w, n) - mn$, and $t = a - \ell o \frac{n + k_2 k_3}{n + k_2}$. The notation f_g with $f = l, h, t$ and $g = w, n, o$, in (6), indicates the derivative of f with respect to the variable g evaluated in the steady state solution (w_0, n_0, o_0).

[17] The steady state is stable if the real part of the growth rate λ is $Re(\lambda) < 0$ and unstable when $Re(\lambda) > 0$. The equation $Re(\lambda) = 0$ identifies the boundary between stable and unstable conditions, is called a critical stability condition and is associated with the critical wave number k_0. Neglecting $\frac{\partial o}{\partial t}$, the critical stability condition of problem (2) was obtained analytically. It is:

$$k_0^2 dn + l_w - k_0^2 + \frac{1}{\sqrt{2}}\left[\left(q^2 + p^2\right)^{1/2} + q\right]^{1/2} = 0, \tag{7}$$

with, $p = 2\, k_0\, v_w\, [l_w - h_n - d_n\, k_0^2\,] - 4\, h_w \frac{l_o t_n v_o k_0}{\left(t_o - k_0^2 d_o\right)^2 + k_0^2 v_o^2}$, and $q = [l_w - h_n - d_n\, k_0^2]^2 + 4[l_n - h_o t_n \frac{t_o - k_0^2 d_o}{\left(t_o - k_0^2 d_o\right)^2 + k_0^2 v_o^2}]\, h_w$.

[18] Equation (7) may be regarded as a relation between any set of model parameters, and defines the boundaries between the stability and instability fields. The latter repre-

Table 2. Model Parameters[a]

Case Study	K_s, m yr^{-1}	D_O, m^2 yr^{-1}	k_3
a	3000	4×10^4	0.1
b	300	4×10^4	0.1
c	3000	4×10^2	0.1
d	3000	4×10^4	0.5

[a]Case studies: a, base; b, reduced soil moisture mobility; c, reduced surface water mobility; d, reduced feedback.

sents the whole set of parameters that leads to the unstable steady state solutions of problem (2).

3. Results

3.1. Stability Field Resulting From Linear Stability Analysis

[19] In Figures 1, 2, and 3 the critical stability condition (equation (7)) is plotted for different values of the parameters k_3, K_s, D_O and i appearing in (2). The linear stability analysis distinguishes between stable and unstable scenarios on the base of the growth rate of a very small disturbance but says nothing about the resulting finite size patterns. Nevertheless, patterns are expected to develop under unstable conditions (within the instability field). Two lines indicate the boundaries of the field of instability where the bands of vegetation are expected to initiate. The lower limit on the left (not labeled), is common to all case studies reported in Figures 1–3; it is $A = 240$ mm yr^{-1} in case 1 and $A = 137$ mm yr^{-1} in case 2. For lower precipitation amounts (below the lower limit of the instability field), no steady state solution, except bare soil, may be found. Above the upper limit of the instability field (for larger A) the steady state solution of the problem is found to be stable, and uniform vegetation cover is expected to establish.

[20] In Figure 1 the critical stability condition (equation (7)) is plotted on the $k_3 - A$ plane for different values of D_0. It is shown that the unstable conditions for the model with $f(w, n) = rwn^2$ (case 1, on the left) did not depend on k_3 and D_0, indicating that neither the feedback mechanism (biomass-dependent infiltration rate), nor the mobility of the surface water were relevant processes in this case. Conversely, the instability field for $f(w, n) = gn\frac{w}{k_1+w}$ becomes smaller for decreasing D_0 and increasing k_3 (case 2, on the right).

[21] In Figure 2 the critical stability condition (equation (7)) is plotted as a relation between K_s and A for different values of D_O. Figure 2 shows that the more mobile the soil moisture (larger K_s values), the larger the A range leading to instability in case 1, whereas the K_s value has minor influence on the stability field in case 2, particularly for large D_O (c). Moreover, increasing K_s for small D_O (b) leads to a restriction of the instability field, as if the increased mobility of soil moisture would have a stabilizing effect on the soil moisture, vegetation and surface water balance. No unstable steady state solution was found for parameter set a in case 2.

[22] Finally, the results obtained in cases 1 and 2 have been compared by plotting the critical stability condition on the A-i plane (Figure 3). Many authors observed that a slope gradient threshold below which no banded pattern develops does exist and that it tends to increase with the mean annual rainfall. By representing the stability condition on the A-i plane, the consistency of the model results with the experimental evidence of a threshold i, may be easily verified. Some of the experimental data published by *Worral* [1960], *Slatyer* [1961], and *Valentin and d'Herbes* [1999] and cited by *Valentin et al.* [1999] are indicated by circles in Figure 3. Each one of them represents the threshold slope gradient of a different catchment. They have been reported to show that a quantitative correspondence between model simulation and experimental data may be achieved, whatever the growth rate, at least by fine tuning parameters, according to *Ursino* [2005]. Figure 3 shows the boundaries of the instability field in four representative situations: base (a), reduced soil moisture mobility (b), reduced surface water mobility (c), and reduced feedback (d). The model parameters have been changed one at a time as indicated in Table 2. The results obtained in case 1 are plotted on the left, those relative to case 2 are plotted on the right.

[23] The results obtained in case study 2 do not show any evidence of a threshold slope gradient increasing with the mean annual rainfall, even though the surface water velocity v_o does depend on the gradient slope and plays a crucial role together with feedback. Increasing surface water mobility beyond the usual literature values could help improve the results, but it would not necessarily lead to a physically based reproduction of the processes in action. Reducing feedback and surface water dispersion narrowed the instability field (cases c and d) whereas reducing K_s (case b) had a minor opposite effect. Case study 1 (Figure 3, left) provided the expected threshold gradient slope that increases with increasing mean annual rainfall A. Nevertheless the soil conductivity had to be stretched beyond its usual range of variability in order to achieve this result, and as a consequence, the physical meaning of this effective parameter becomes questionable. In case study 1 the rainfall range where instability was predicted was restricted to the lower A values for smaller K_s (b), whereas decreasing D_O or increasing k_3 (c and d) left the results substantially unchanged. In summary, soil moisture diffusion affects the equilibrium of biomass density for quadratic biomass growth and has negligible effect on linear biomass growth, according to *Klausmeier* [1999]. In contrast, feedback induces pattern formation under the hypothesis of linear biomass growth, as demonstrated by *HilleRisLambers et al.* [2001], whereas for quadratic biomass growth, the impact of feedback is minor.

[24] In case study 3.1 and 3.2, substituting $f(w, n)$ within the differential problem (2) and evaluating (7) with $K_s = 300 \div 3000$ m yr^{-1}, $D_O = 4 \div 4 \times 10^4$ m^2 yr^{-1}, $i = 0 \div 0.02$, and $k_3 = 0.1 \div 0.5$, provided stable steady state solution of (2) irrespectively of A. One may be keen to infer that the mechanisms that initiate the formation of vegetation bands have nothing to do with the competitive growth that motivates the logistic equation but rather that they are linked to pioneering colonization or plant cooperation. Indeed, reasonably, mutual aid promotes banding whereas competition restrains it, unless self-inhibitory interactions act over long distances, whereas cooperative interaction take place over short distances as simulated by *Lefever and Lejeune* [1997].

3.2. Long-Term Numerical Solution

[25] In this section the discussion is restricted to case study 1 and 2, that led to instability of problem (2) by

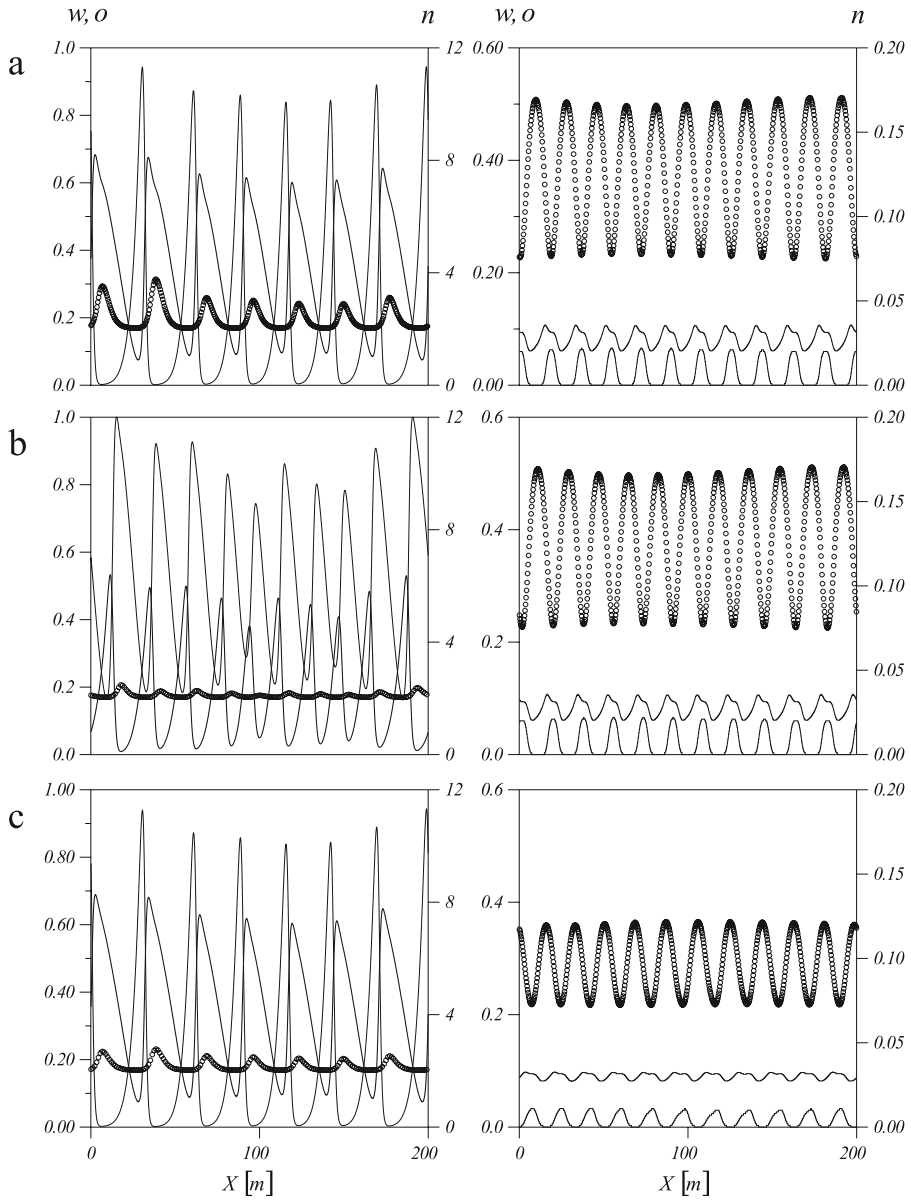

Figure 4. Long-term solution of problem (1). Thick line, dimensionless soil moisture w (left axes); thin line, dimensionless biomass n (right axes); circles, dimensionless surface water o (left axes). (left) Case study 1. (right) Case study 2. (a) Base, (b) reduced soil moisture diffusion, and (c) reduced feedback. Periodic boundary conditions are used. Parameter values are reported in Table 3.

mimicking local plant cooperation. Although it may seem reasonable that the vegetation organization be initially favored by local plant cooperation and thus that the growth rate may initially increase with biomass density, as soon as the population increases, some additional self regulating mechanism is expected to take place. The linear stability analysis focuses on the banding initiation and thus the results presented in section 3.1 are not in contrast with the above statement. However, the long time solution of problem (2) may be questionable in case study 1 and 2. Indeed, the results of the numerical integration are shown here just to explain the fact that there are hydrological processes that have minor effects on the results of the stability analysis depending on the biomass growth rate. In other words, the analysis of the long-term solution should clarify the interrelation between plant physiology and relevant hydrological processes that were deduced by the results of the linear stability analysis, rather than advance the comprehension of the real long-term behavior of banded vegetation patterns and the related soil moisture distribution. Assuming, as an

Table 3. Model Parameters[a]

Case Study	Case 1			Case 2		
	A, mm yr^{-1}	K_s, mm yr^{-1}	k_3	A, mm yr^{-1}	K_s, mm yr^{-1}	k_3
a	245	3000	0.1	150	3000	0.1
b	245	1000	0.1	150	300	0.1
c	245	3000	0.5	150	3000	0.2

[a]Case studies: a, base; b, reduced soil moisture mobility; c, reduced feedback.

initial condition, the superposition of an unstable homogeneous steady state solution and a small heterogeneous perturbation (gaussian noise), problem (2) has been solved numerically to derive the soil moisture, biomass and surface water spatial distribution after a long simulation time.

[26] In Figure 4 the results of numerical integration of (2) are plotted for different values of A, K_s and k_3. Input data have been reported in Table 3. The results of case study 1 are plotted on Figure 4 (left); those of case 2 are plotted on Figure 4 (right). The three scenarios that have been considered are base (Figure 4a), reduced soil moisture mobility (Figure 4b), and reduced feedback (Figure 4d). All data refer to time $T = 20$ years, when the soil moisture and the biomass density display "a kind of stationary behavior." Indeed, in accordance with the experimental observation, the bands migrate along the slope, and the long time results are stationary only in a moving reference system.

[27] In all cases maximum biomass and minimum surface water coincided demonstrating that the model mimics the mechanism of surface water redistribution from bare soil toward vegetated by runoff.

[28] In case 1 (Figure 4, left) the interband soil was found to be unexpectedly wetter than the vegetated soil, whereas in case study 2 (Figure 4, right), the soil moisture was reasonably minimum in between the bands. In all cases, the absolute maximum soil moisture resulted in a slight shift in respect to the maximum vegetation density, evidencing that soil moisture may accumulate at the edges of the vegetated zones.

[29] The results shown in Figure 4 explain why soil conductivity counted so much in the stability analysis of case 1: plants need a large amount of water, due to their high density and due to the quadratic dependence of the growth rate on the biomass density. Thus they use soil moisture that infiltrates locally but also soil moisture that infiltrates in the interband and since the plant roots do not extend to the interbands (according to the model assumptions), their survival depends on the gradient between band and interband saturation and on the soil conductivity. Under these circumstances, obviously, the feedback counts less. It is evident that plant physiology is badly represented in this case by the model. In case 2, the vegetation uses only part of the soil moisture infiltrating preferentially on the vegetated surface and that is stored in the band root zone. Higher lateral conductivity would eventually disperse the scarce resource and thus would not favor the vegetation organization.

4. Discussion and Conclusions

[30] There are many unexploited aspects of the intriguing phenomenon of vegetation pattern formation. This study points at the interrelation between the dynamic of plant growth and the hydrological processes involved. Important hints emerged from the results of linear stability analysis of a simple model for soil moisture, vegetation and surface water balance.

[31] 1. The local cooperative interaction among plants proved crucial for vegetation banding, in accordance with previous published results. Indeed, the logistic equation, that expresses competition among plants instead of plant synergy, in the experiments reported here did not lead to any unstable steady state, no matter how much the hydrological processes favored the vegetation banding. Nevertheless, the consistency of results obtained with growth rates based on plant cooperation (nondecreasing growth rate with increasing density) was demonstrated to be controversial.

[32] 2. Different processes had an impact on the equilibrium of our model (2) depending on how fast the relative growth rate increased with biomass density and soil moisture. In case 1 ($f(w, n) = rwn^2$) the stability field of (2) was more sensitive to soil moisture redistribution. In case 2 ($f(w, n) = gn \frac{w}{k_1 + w}$) feedback and surface water redistribution had a major influence on the stability field, whereas soil moisture mobility, in contrast with case 1, had a minor stabilizing effect. The long-term solution of problem (2) demonstrated that the soil moisture distribution linked to the band formation, is substantially different in cases 1 and 2. In case 1 soil moisture accumulated in the interband zone, in case 2 it accumulated in the vegetated band soil. Whether the model mimics the natural hydrological fluxes is questionable. Indeed, plant roots are expected to develop in order to compensate for local lack of resources in more saturated adjacent zones, adapting to the environmental conditions. The model however, is based on the assumption that soil moisture uptake is a point process. More realistically, in case 1, uptake should be modeled as a distributed outflow from the places where soil moisture accumulates and toward which the roots grow. This further modeling exercise was beyond the scope of this paper.

[33] It has been demonstrated here that defining how fast plants grow depending on plant density and soil moisture availability in arid and semiarid environments is a fundamental issue, and certainly deserves further thoughtful investigation. Indeed, the amount of water that plants use and their growth rate, determine which hydrological processes enable the formation of vegetation patterns and could be a crucial point, e.g., in restoration projects of degraded lands or when searching an optimum distribution of cultivated plants in catchments characterized by scarce resources. Similar to the majority of studies that focus on soil moisture and biomass balance stability, a detailed spatial resolution was not used for root growth and moisture uptake, and thus they probably were not always represented with the necessary care (they were certainly not in case study 1). Since the soil-vegetation interaction at the root level is extremely important, this lack of accuracy risks inducing completely misleading conclusions regarding the relevance of the effect that different hydrological processes have on the formation of vegetation patterns. Furthermore, although all models mimic just partially how nature behaves, it is unclear which one gives a more realistic prediction of the relevant hydrologic processes in action. The most reasonable conclusion seems to warrant envisioning the need for more accurate models for the soil-vegetation-atmosphere continuum in order to predict relevant hydrologic processes and set up more predictive tools for early warning of catastrophic shift and restoration of degraded lands.

References

Berryman, A. A. (1992), Intuition and the logistic equation, *Trends Ecol. Evol.*, *7*, 316.

Boaler, S. B., and C. A. H. Hodge (1962), Vegetation stripes in Somaliland, *J. Ecol.*, *50*, 465–474.

Boaler, S. B., and C. A. H. Hodge (1964), Observations on vegetation arcs in the northern region Somali Republic, *J. Ecol.*, *52*, 511–544.

Fernando, T. M., and J. Cortina (2002), Spatial patterns of surface soil properties and vegetation in a Mediterrean semi-arid steppe, *Plant Soil*, *241*, 279–291.

Gabriel, J.-P., F. Saucy, and L.-F. Bersier (2005), Paradoxes in the logistic equation?, *Ecol. Modell.*, *185*, 147–151.

Gardner, W. R. (1958), Some steady state solution of the unsaturated soil moisture flow equation with application to evaporation from a water table, *Soil Sci.*, *85*(4), 228–232.

Gilad, E., J. von Hardenberg, A. Provenzale, M. Shachak, and E. Meron (2004), Ecosystem engineering: From pattern formation to habitat creation, *Phys. Rev. Lett.*, *93*, 098105.

HilleRisLambers, R., M. Rietkerk, F. van den Bosch, H. H. T. Prins, and H. de Kroon (2001), Vegetation pattern formation in semi-arid grazing systems, *Ecology*, *82*(1), 50–61.

Klausmeier, C. A. (1999), Regular and irregular patterns in semiarid vegetation, *Science*, *284*, 1826–1828.

Lefever, R., and O. Lejeune (1997), On the origin of tiger bush, *Bull. Math. Biol.*, *59*(2), 263–294.

Murray, J. D. (1989), *Mathematical Biology*, Springer, New York.

Olson, M. H. (1992), Intuition and the logistic equation, *Trends Ecol. Evol.*, *7*, 314.

Richards, L. A. (1931), Capillary conduction of liquids through porous medium, *Physics*, *1*, 318–333.

Rietkerk, M., F. van den Bosch, and J. van de Koppel (1997), Site-specific properties and irreversible vegetation changes in semi-arid grazing systems, *Oikos*, *80*, 241–252.

Rietkerk, M., S. Dekker, P. C. de Ruiter, and J. van de Koppel (2004), Self-organized patchiness and catastrophic shifts in ecosystem, *Science*, *305*, 1926–1929.

Rodriguez-Iturbe, I., A. Porporato, L. Ridolfi, V. Isham, and D. R. Cox (1999), Probabilistic modelling of water balance at a point: The role of climate, soil and vegetation, *Proc. R. Soc. Lond., Ser. A*, *455*, 3789–3805.

Salvucci, G. D. (2001), Estimating the moisture dependence of root zone water loss using conditional averaging precipitation, *Water Resour. Res.*, *37*(5), 1357–1365.

Slatyer, R. O. (1961), Methodology of water balance study conducted on a desert woodland community in central Australia, in *Plant-Water Relationships in Arid and Semi-Arid Conditions: Proceedings of the Madrid symposium*, *Arid Zone Res*, vol. 16, pp. 15–25, U. N. Educ., Sci., and Cultural Organ., Paris.

Tongway, D., and J. A. Ludwig (1990), Vegetation and soil patterning in semi-arid mulga lands of eastern Australia, *Aust. J. Ecol.*, *15*, 23–34.

Tsoularis, A., and J. Wallace (2002), Analysis of logistic growth models, *Math. Biosci.*, *179*, 21–55.

Turing, A. M. (1952), *Philos. Trans. R. Soc. London, Ser. B*, *237*, 37.

Ursino, N. (2005), The influence of soil properties on the formation of unstable vegetation patterns on hillsides of semiarid catchments, *Adv. Water Resour.*, *28*, 956–963.

Ursino, N., and S. Contarini (2006), Stability of banded vegetation patterns under seasonal rainfall and limited soil moisture storage capacity, *Adv. Water Resour.*, *29*, 1556–1564.

Valentin, C., and J. M. d'Herbes (1999), Niger tiger bush as a natural water harvesting system, *Catena*, *37*, 231–256.

Valentin, C., J. M. d'Herbes, and J. Poesen (1999), Soil and water components of banded vegetation patterns, *Catena*, *37*, 1–24.

Verhulst, P. F. (1838), Notice sur la loi que la population suit dans son accroissement, *Corr. Math. Phys.*, *10*, 113–117.

Von Hardenberg, J., E. Meron, M. Shachak, and Y. Zarmi (2001), Diversity of vegetation patterns and desertification, *Phys. Rev. Lett.*, *87*, 198101.

White, L. P. (1970), Brousse tiger patterns in southern Niger, *J. Ecol.*, *58*, 549–553.

White, L. P. (1971), Vegetation stripes on sheet wash surfaces, *J. Ecol.*, *59*, 615–622.

Worral, G. A. (1959), The Butana grass patterns, *J. Soil Sci.*, *10*, 34–53.

Worral, G. A. (1960), Patchiness in vegetation in the northern Sudan, *J. Ecol.*, *48*, 107–117.

Young, T. P. (1992), Intuition and the logistic equation, *Trends Ecol. Evol.*, *7*, 315–316.

N. Ursino, Department IMAGE, University of Padova, Via Loredan, 20, I-35131 Padova, Italy. (nadia@idra.unipd.it)